Sterol Methyltransferase: Functional Analysis of Highly Conserved Residues by Site-Directed Mutagenesis†

W. David Nes,*,‡ Pruthvi Jayasimha,‡ Wenxu Zhou,‡ Ragu Kanagasabai,‡ Changxiao Jin,§ Tahhan T. Jaradat,‡ Robert W. Shaw,‡ and Janusz M. Bujnicki||

Department of Chemistry and Biochemistry, Texas Tech University, Lubbock, Texas 79409-1061, and Bioinformatics Laboratory, International Institute of Molecular and Cell Biology, Trojdena, 4 02-109 Warsaw, Poland

Received July 16, 2003; Revised Manuscript Received November 10, 2003

ABSTRACT: Sterol methyltransferase (SMT), the enzyme from *Saccharomyces cerevisiae* that catalyzes the conversion of sterol acceptor in the presence of AdoMet to C-24 methylated sterol and AdoHcy, was analyzed for amino acid residues that contribute to *C*-methylation activity. Site-directed mutagenesis of nine aspartate or glutamate residues and four histidine residues to leucine (amino acids highly conserved in 16 different species) and expression of the resulting mutant proteins in *Escherichia coli* revealed that residues at H90, Asp125, Asp152, Glu195, and Asp276 are essential for catalytic activity. Each of the catalytically impaired mutants bound sterol, AdoMet, and 25-azalanosterol, a high energy intermediate analogue inhibitor of *C*-methylation activity. Changes in equilibrium binding and kinetic properties of the mutant enzymes indicated that residues required for catalytic activity are also involved in inhibitor binding. Analysis of the pH dependence of log k_{cat}/K_m for the wild-type SMT indicated a pH optimum for activity between 6 and 9. These results and data showing that only the mutant H90L binds sterol, AdoMet, and inhibitor to similar levels as the wild-type enzyme suggest that H90 may act as an acceptor in the coupled methylation−deprotonation reaction. Circular dichroism spectra and chromatographic information of the wild-type and mutant enzymes confirmed retention of the overall conformation of the enzyme during the various experiments. Taken together, our studies suggest that the SMT active center is composed of a set of acidic amino acids at positions 125, 152, 195, and 276, which contribute to initial binding of sterol and AdoMet and that the H90 residue functions subsequently in the reaction progress to promote product formation.

Sterol *C*-methylations catalyzed by the fungal sterol methyltransferase (SMT;[1] EC 2.1.1.41) have provided the focus for the study of electrophilic alkylations, a reaction type of functional importance in C−C bond formation of phytosterols (*1*−*3*). *ERG*6 encodes the yeast SMT, which has been cloned, overexpressed in *Escherichia coli*, and purified to homogeneity (*4*−*6*). The fungal ability to *C*-methylate sterols is the only proven difference in sterol synthetic pathways between humans and opportunistic pathogens; as such, the SMT is considered to be a unique target for rational drug design (*7*−*9*). Cultures of *Saccharomyces cerevisiae*, *Candida albicans*, or *Gibberella fujikori* in the presence of SMT inhibitors such as 25-azalanosterol **5** result in the decreased production of ergosterol **4**, the accumulation of zymosterol **2**, and the inhibition of growth, supporting its identification as a critical step (Scheme 1) (*10*−*15*).

The deduced sequences of *ERG*6 and other members of the SMT family from fungi and plants (Supporting Information) share a high degree of similarity (*16*) and contain conserved polar residues that can contribute to a common order of events and intermediates involved in the catalytic process. The fundamental similarities among SMT primary structures are also reflected in the apparent similarities in overall steady-state parameters, molecular weight, and subunit organization (*1*, *17*), suggesting a common topography in the active center. Further evidence favoring a similar three-dimensional arrangement of related amino acids in the active center of diverse SMT enzymes is the covalent labeling of these proteins with a methylenecyclopropane analogue of the native substrate zymosterol or cycloartenol (*18*, *19*). Using enzyme redesign to address whether substrate channeling can be directed (*19*, *20*), Nes et al. discovered that substitution of a leucine residue for the highly conserved glutamate residue 82 in the yeast SMT sterol binding site signature motif (region I, residues 81−91) generated a mechanistically decoupled enzyme to give a product set analogous to that generated by some plant SMTs (*19*). In view of the importance of an acidic residue to the catalytic pathway, 13 highly conserved polar residues were substituted

† This work was supported by NIH Grant (GM 63477), NSF Grant (MCB 0115401), and Welch Grant (D-1276) to W.D.N. J.M.B. is supported by the EMBO/HHMI Young Investigator Program Award and by a Young Investigator Fellowship from the Foundation for Polish Science.

* To whom correspondence should be addressed. Tel: (806) 742-1673. Fax: (806) 742-0135. E-mail: wdavid.nes@ttu.edu.

‡ Texas Tech University.

§ Current address: The Third Affiliated Hospital, Heath Science Center of Peking University, Beijing 100083, P. R. China.

|| International Institute of Molecular and Cell Biology.

[1] Abbreviations: SMT, sterol methyltransferase; CD, circular dichroism; GC−MS, gas chromatography−mass spectroscopy; BSA, bovine serum albumin; AdoMet, *S*-adenosyl-L-methionine.

10.1021/bi035257z CCC: $27.50
Published on Web 12/20/2003

Scheme 1: Lanosterol−Ergosterol Pathway and Blockage by 25-Azalanosterol

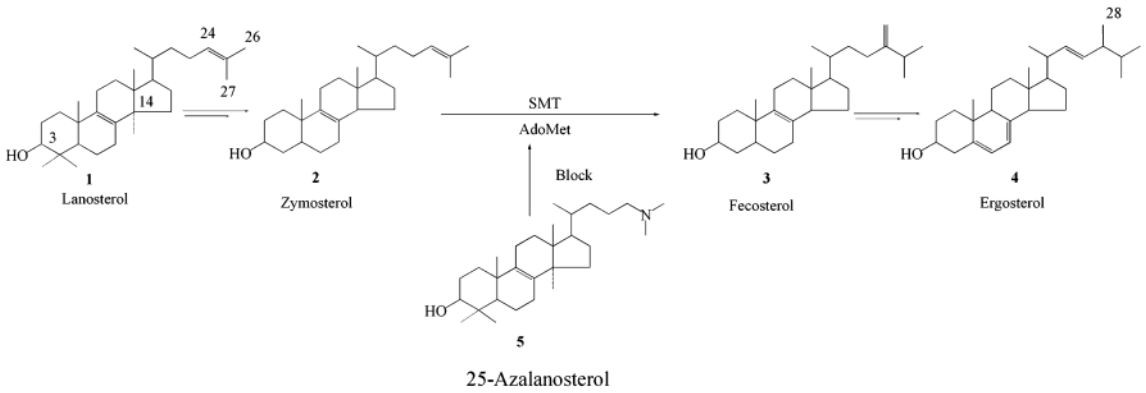

with leucine, and the biochemical effects were determined in relation to possible conformational changes in the recombinant proteins as revealed by circular dichroism and gel-permeation chromatography. In addition, the kinetics and binding behavior of 25-azalanosterol, a high energy intermediate of the *C*-methylation pathway (*9*, *10*), have been investigated, and a comparative structural evaluation based on homology modeling and impaired SMT action with implications for the recognition of substrate features to SMT catalysis was determined.

EXPERIMENTAL PROCEDURES

Materials. The sources and preparation of substrates zymosterol, [3-^{3}H]zymosterol (sp. act. 9 μCi/μmol) 25-azalanosterol, [3-^{3}H]25-azalanosterol (sp. act. 99 μCi/μmol), AdoMet iodide salt, and *S*-[methyl-$^3H_3$]adenosyl-L-methionine (NEN, diluted with AdoMet to a sp. act. of 10 μCi/μmol) were as described in our preceding papers (*19*, *21*). The Bradford protein assay kit and protein electrophoresis supplies were purchased from Bio-Rad. IPTG was purchased from Research Products International Corp. Reagents and chemicals used in growing bacteria, enzyme purification, and assays were purchased from Sigma and Fisher unless otherwise noted.

General Methods. General methods for sterol analyses, heterologous expression, and homogenate preparation and analyses were as described (*6*). Protein concentration containing the crude SMT enzyme was determined by the Bradford method (*22*) with bovine serum albumin (BSA) as a standard using commercial reagents from Bio-Rad. Otherwise, the determination of pure SMT concentration was measured at A_{280} using an extinction coefficient of, for example, 58 370 M^{-1} cm^{-1} for native SMT. Extinction coefficients for the mutants were similar to the wild-type value. GC−MS analysis of enzyme-generated products was performed with a Hewlett-Packard 6890 GC interfaced to a 5973 mass spectrometer (Palo Alto, CA). The fused silica capillary column was 30 m × 250 μm i.d. coated with a 0.25 μm film of DB-5 (Agilent technology, Palo Alto, CA) and was programmed from 170 to 280 °C at 20 °C/min with He gas flow at 1.2 mL/min. The MS operating parameters were ionization voltage, 70 eV (electron ionization) and interface temperature, 250 °C.

Protein Purification of Wild-Type and Mutant SMTs. In an earlier study, we purified the cloned SMT after overexpression of the enzyme in *E. coli* (*6*). We have improved on the purification method by reducing the number of steps and time involved in the purification of SMT, thereby increasing the enzyme activity and doubling the overall yield of protein as compared to our earlier protocol. Briefly, a frozen stock of the BL21(DE3) strain harboring the yeast SMT or mutated yeast SMT cDNA provided single colonies to inoculate 250 mL of Luria−Bertani medium containing ampicillin (50 μg/mL) and grown for 10 h at 37 °C in a floor shaker. The culture was used to inoculate 2 L of Luria broth divided into four Erlenmeyer flasks containing the same antibiotic. When A_{600} of the suspended culture reached ca. 0.5, isopropyl-1-thio-β-D-galactopyranoside was added to a final concentration of 0.4 mM, and the culture was incubated further at 37 °C for 2 h with moderate shaking (200 rpm) to induce protein expression. The cells were pelleted by centrifugation (4 °C, 10 000*g*, 10 min), and the cell paste was snap frozen with liquid nitrogen and stored at −80 °C or used directly. The cell paste (5 g) was resuspended in 30 mL of buffer A (50 mM Tris-HCl, 2 mM $MgCl_2$, 2 mM β-mercaptoethanol, 1 mM EDTA, and 5% glycerol (v/v) at pH 7.5), and the suspension was lysed by passage through a French pressure cell at 20 000 psi. Insoluble protein and cell debris were removed by centrifugation (4 °C, 100 000*g*, 1 h), and the supernatant (25 mL) was used for enzyme assay or as a source of protein for further purification. All procedures were carried out at 4 °C. To reduce contaminants, the 100 000*g* supernatant was applied to a column of Q sepharose (ca. 20 nmol of protein to 20 mL column volume) preequilibrated with buffer A. To the first 25 mL of eluant was added 0.4% emulphogen, and the sample was stirred on ice for 30 min. The material was loaded onto a Q sepharose column containing buffer A and emulphogen detergent (to a final concentration of 0.4%). The column was developed stepwise gradient from 0.1 to 1 M NaCl in buffer A and detergent (0.4%). Each fraction (30 mL/15 min) was monitored for SMT activity for wild-type SMT and active mutant or by SDS−PAGE gel electrophoresis. Protein content during the purification was estimated by the method of Bradford referenced to BSA. Fractions corresponding to 0.20 M salt (or 0.25 M salt for the mutant) containing the target protein were combined, desalted by washing with fresh buffer A (15 × 5 mL), and concentrated (Amicon ultrafiltration YM-10 membrane) to a final volume of 10 mL. The average yield to this point was ca. 50 mg of total protein of which about 85% represented SMT. The solution from Q sepharose was loaded onto a Pharmacia Mono Q HR 10/10

column that was previously equilibrated with buffer A containing 0.4% emulphogen. The column was eluted with a 150 mL stepwise gradient from 0.050 to 0.5 M NaCl in the same buffer while monitoring the effluent as before. A set of highly active fractions (2 mL each) in 0.20 M NaCL (or 0.25 M NaCl for the mutant) possessed a homogeneous protein by SDS−PAGE (single ca. 43 kDa band). The amount of SMT recovered at this stage of purification was about 10 mg.

Molecular Weight Determination. Native molecular weight of pure WT protein and H90L protein from FPLC was determined by gel-permeation chromatography. A 2.5 mg sample of pure protein in 0.4% emulphogen was loaded onto a calibrated (Bio-Rad reference standards from 1.67 to 670 kDa) HiprepTM 26/60 Sephacryl S-300 high resolution gel filtration column (Pharmacia) coupled to an FPLC system eluted at a flow rate of 1 mL/min with 0.1 M NaCl in buffer A. For wild-type enzyme, activity assays were performed on each fraction during the run from 10 to 300 min to identify the target protein eluted from the column; alternatively, inactive mutant (H90L) was monitored by SDS−PAGE with native SMT as the chromatographic reference specimen (M_r, 43 kDa). In all cases, a single protein elution peak was observed between fractions 130 to 140 min, which corresponded to a calculated molecular weight of ca. 172 kDa.

SMT Assays and Product Distribution. The standard assay for enzyme activity was performed in 600 μL of total volume, 5−15 μg of pure protein, or 1−2 mg of total protein in buffer B (50 mM Tris-HCl buffer, 2 mM $MgCl_2$, 2 mM 2-mercaptoethanol, and 20% (v/v) glycerol, pH 7.5), 50 μM sterol substrate, 50 μM [methyl-$^3H_3$]AdoMet at 0.6 μCi and Tween 80 (0.1%, v/v) to produce 10^4−10^6 dpm of product in 45 min at 32 °C. The incubation mixture was terminated with 500 μL of a solution of 10% methanolic KOH. The methylated sterol product was extracted three times with 2.5 mL each in hexane (Fisher) and mixed on a vortex mixer for 30 s. The resulting organic layer was transferred to a 10 mL scintillation vial and dried, and the sample was analyzed by liquid scintillation counting to determine the conversion rate. For kinetic analysis, standard assays were performed at 10 substrate concentrations from 5 to 200 μM sterol with the AdoMet concentration held at saturation of 50 μM. From the variation of reaction velocity with substrate concentration according to Michaelis−Menten kinetics, an apparent saturation of either substrate approached 50 μM (data not shown). Random variations in measured velocities did not exceed ±10%. For native protein, reactions up to 3 h were linear with a protein concentration up to 2 mg/mL, and for product distribution measurements, overnight assays at saturating concentrations of substrates generated about 70% conversion of zymosterol to fecosterol. The initial velocity data were determined using the computer program Sigmaplot 2001 plus the enzyme kinetics module software package. Data were fitted to the equation, $v = V_{max}S/(K_m + S)$, using a nonlinear least-squares approach. Kinetic constants ± standard errors (SE) were never greater than 5% of the experimental measurement, and R^2 values were between 0.95 and 0.97. The nature and yield of the enzyme-generated product was determined by GC−MS of the nonsaponifiable lipid fraction from activity assays allowed to incubate overnight.

Site-Directed Mutagenesis of SMT. Point mutations were generated using the QuikChange site-directed mutagenesis kit (Stratagene) according to the manufacturer's instruction. Oligonucleotide sequences of mutagenic primers are listed in Table 1.

Table 1: DNA Sequence of the Synthetic Oligonucleotides Used for the Site-Directed Mutagenesis of the *ERG6* Gene[a]

Mutation	Sense oligonucleotide sequence (5'-3')
His90Leu	5′-TGGGGTTCCTCTTTCCTTTTCAGCAGATTTTAT-3′
His107Leu	5′-CTGCCTCGATAGCAAGACTTGAACATTATTTAGCTTA-3′
Glu108Leu	5′-TGCCTCGATAGCAAGACATCTACATTATTTAGCTTACAAGG-3′
Asp125Leu	5′-AAGAGGCGATTTAGTTCTCCTCGTTGGTTGTGGTGTTGGG-3′
Asp152Leu	5′-TCGGTCTAAACAATAACCTTTACCAAATTGCCAAGGGC-3′
Asp189Leu	5′-GAAGAAAACACTTTCTTCAAAGTTTATGCAATTG-3′
Glu195Leu	5′-GACAAAGTTTATGCAATTCTGGCCACATGTCACGCTCCA-3′
His199Leu	5′-ATTGAGGCCACATGTCTCGCTCCAAAATTAGAA-3′
Glu209Leu	5′-AATTAGAAGGTGTATACAGCCTAATCTACAAGGTTTTGAAACC-3′
Glu224Leu	5′-GGTACCTTTGCTGTTTACCTATGGGTAATGACTGATAAA-3′
His238Leu	5′-ACGAAAACAATCCTGAACTTAGAAAGATCGCTTATGA-3′
Glu246Leu	5′-AAAGATCGCTTATGAAATTCTACTAGGTGATGGTATCCCA-3′
Asp276Leu	5′-GTCCTCGTTAGCGAACTCCTGGCGGACAATG-3′

[a] Codons for the changed amino acids are underlined.

Binding Assays and Immunoblotting. To determine the dissociation constant (K_d) for zymosterol, AdoMet, and 25-azalanosterol, filter ligand-binding assays were performed as described elsewhere (*20*). Purified wild-type and mutant protein preparations were used in these experiments. The binding assays were performed by the filter-binding method in 0.2 mL volumes of buffer A (50 mM Tris-HCl, 2 mM $MgCl_2$, 1 mM EDTA, 2 mM β-meracptoethanol, and 5% glycerol, pH 7.5) at 32 °C and incubated for 2 h in a shacking water bath. Free ligands were separated from the protein−ligand complex on 2.5 cm diameter GF/B glass fiber filter disks (Whatman) with a slight applied vacuum. The filters were pretreated with a solution of 0.1% BSA to block nonspecific binding to the filters and washed three times with 1 mL of ice-cold buffer A each. The disks were then air-dried, and the adhering radioactivities were determined using a Beckman LS6000 liquid scintillation counter. The molar concentration of ligand bound to the protein was calculated from the experimentally determined radioactivities, and the corresponding concentrations were fitted into a one site saturation ligand binding equation of $Y = (B_{max}X)/(K_d + X)$, where Y is the concentration of the ligand specifically bound to the protein, B_{max} is the maximum number of binding sites, and X is the total ligand concentration including the protein-bound ligand. The amounts of the three ligands used ranged between 0.24 and 28.0 μM for [3-^{3}H]zymosterol, 0.38 to 16.0 μM for [3-^{3}H]25-azalanosterol, and 0.04 to 3.76 μM for [methyl-$^3H_3$]AdoMet. Protein concentrations were determined by the Bradford method. A typical binding isotherm for 25-azalanosterol that has reacted with native SMT is shown in Figure 1. Calculation of the $\Delta G_{binding}$ values is based on the tetramer organization of the SMT and the formula $\Delta G = RT \ln K_d$ (*23*). For immunoblotting, either crude or pure SMT were electroblotted onto nitrocellulose membranes, and a duplicate SDS−PAGE gel (12%) was stained with Coomassie blue. Blots were developed with a polyclonal antibody raised against yeast SMT (*6*), as primary antibody and goat antibody IgG conjugated to alkaline phosphatase as secondary antibody. The color was developed with an alkaline phosphatase substrate kit (Bio-Rad) for the desired time.

pH Profile Analysis. About 70 mg of protein recovered from the Mono Q column in 50 mM Tris-HCl buffer was precipitated by incubating with 50% PEG (3350) at 4 °C for 30 min. Precipitated protein was recovered by centrifuga-

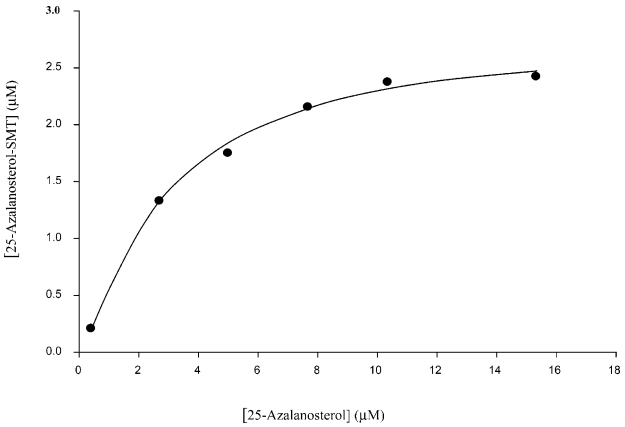

FIGURE 1: Langmuir isotherm for the determination of the dissociation constant (K_d) for 25-azalanosterol bound to the *S. cerevisiae* SMT. Equilibration was performed by the filter binding method as described under Experimental Procedures.

tion at 25 000*g*. The protein pellet was washed with fresh 0.1 M phosphate buffer at the desired pH value twice and dissolved in 10 mL of the same phosphate buffer. After exchanging the buffers (Tris-HCl to phosphate), enzyme assays at each of the pH values were performed concurrently to determine the SMT activity, and K_m and k_{cat} values were determined as described (*20*). The pH values of the phosphate medium were performed over a range between pH 3 and 10. To ensure that reactions are performed at the intended pH values, [methyl-$^3H_3$]AdoMet and sterol were also prepared at the intended final buffer pH. Triplicate activity assays were performed at 5, 10, 15, 20, 25, 50, and 100 μM zymosterol and 50 μM total AdoMet, and minimal variation was detected in the experimentally determined kinetic constants with standard errors of 5−10%.

Circular Dichroisim Analyses. Far-UV CD spectra were recorded at 25 °C with a Olis Model DSM-1000 circular dichroism spectrometer using a 1 mm path length quartz cell. CD spectra were recorded at 180−250 nm using a spectral bandwidth of 1.0 nm. Wild-type and mutant SMT obtained from the Mono Q column was transferred to a 10 mM phosphate buffer, pH 7.5 to remove the Tris-HCl that affected protein aggregation during concentration. Thus, a set of dialysis exchanges was employed using 3 mL of Slide-A-Lyzer cassettes (Pierce). Protein in buffer A was dialyzed three times against 500 mL of distilled water with 5% glycerol at 4 °C and continuous stirring for 3 h each. Proteins were then dialyzed against 500 mL volumes of 10 mM phosphate buffer, pH 7.5 at 4 °C and continuous stirring for 3 h each. The activity of the wild-type protein was measured after the buffer exchange process and showed no dramatic reduction of SMT activity, consistent with a retention of the native protein conformation. CD spectra were recorded using a solution of 2 μM SMT, and the spectra were converted to molar elliptcity [θ] prior to analysis. Secondary structure determination based on the CD analysis of the native and mutant SMTs was estimated using software with a reference set of 29 proteins from the CDSSTR program (*24*).

Homology Modeling of SMT. The structure of the SMT was predicted using the Meta Server gateway (the collection of links and literature references to the individual secondary structure prediction and fold-recognition methods is provided on the website http://genesilico.pl.meta/). Known crystallographic structures of related AdoMet-dependent methyltransferase (ref *25* and references therein) were used as modeling templates. The modeling followed the Frankenstein's Monster protocol (*26*, *27*).

RESULTS AND DISCUSSION

Site-Directed Mutagenesis of Acidic Amino Acids. In earlier studies, using a series of substrate analogues that differed from the native substrate in a specific moiety or group of atoms, we developed a steric−electric plug model to indicate possible interactions between SMT and sterol substrate during catalysis (*16*, *28*, *29*). According to the stereochemical model, the C-3 hydroxyl group and Δ^{24}-bond of the sterol acceptor molecule are essential features to binding, and *C*-methylation proceeds via a noncovalent pathway whereby methyl addition to the *Si*-face of Δ^{24} and deprotonation of C-28 give rise to a nucleophilic rearrangement in which H-24 migrates to C-25 on the *Re*-face of the substrate double bond in concert with the initial ionization. In related studies, aimed at reshaping the enzyme specificity and mechanism, we modified the signature motif region I generating a Y81F mutant that resulted in a gain-in-function. The Y81F mutant performed like a plant SMT by catalyzing the transfer of two methyl groups from AdoMet to the sterol Δ^{24}-bond (*20*). A second mutant, generated in region I at position E82, was also found to perform like a plant SMT, albeit differently, catalyzing in the first C_1-transfer reaction a $\Delta^{24(28)}$ —as well as a $\Delta^{25(27)}$—olefin product (*19*). Since reaction channeling was observed after the activity assay of the E82 mutant to give two products, we concluded the acidic amino acid must be on the *Re*-face of the substrate double bond undergoing *C*-methylation by AdoMet.

The E82 residue in the wild-type enzyme was not likely to be ionized, otherwise it would capture H-24 during the 1,2-hydride shift to C-25 during the catalytic reaction. The possibility that some other acidic residue was (i) playing dual roles in the active center as a counterion to AdoMet and as a deprotonating agent involved with the coupled methylation−deprotonation reaction (*30*, *31*), (ii) acting as a base involved with hydrogen bonding to AdoMet or the nucleophilic groups on the sterol at either the C-3 hydroxyl group or the C-24(25) double bond (*28*, *32*), or (iii) directing reaction channeling to form novel products (*19*, *20*) prompted us to consider mutating the remaining highly conserved acidic residues in the wild-type SMT.

Information regarding the most likely amino acid units for substrate recognition at C-3 and Δ^{24} and in the catalytic cycle involving deprotonation of C-28 was obtained from site-specific mutagenesis of aspartate and glutamate residues of the enzyme that are conserved in 16 different species that cross evolutionary lines from fungi to plants (cf. Supporting Information). Mutant forms that retain some or all of the original activity were characterized by a combination of steady-state kinetic analysis, equilibrium dialysis, and GC−MS analyses of the enzyme-generated products and by means of measuring protein conformation by a combination of CD spectroscopy and gel-permeation chromatography to distinguish unambiguously between trivial mutations that cause loss of activity through the loss of substrate binding or those that involve catalytically essential residues. We hypothesized that for an amino acid to function in ligand interaction or as

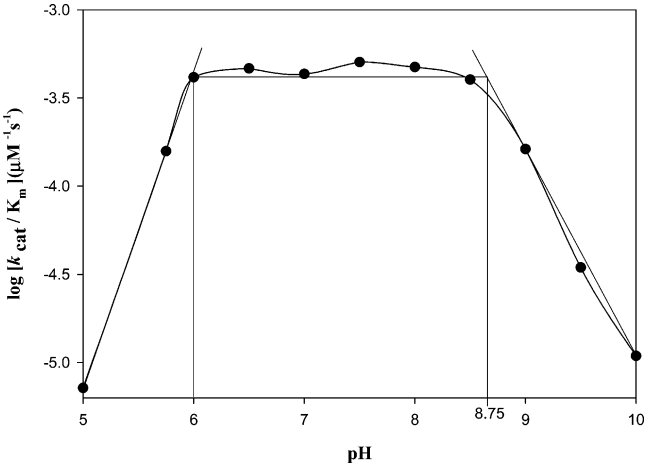

FIGURE 2: pH dependence of sterol *C*-methylation catalyzed by wild-type SMT. Activity assays were performed in phosphate buffer of varied pH. Each data point represents the mean of three measurements with standard errors of 5−10%. The pK_{a1} and pK_{a2} of the protein were determined from the convergent points to be 6.0 and 8.8, respectively.

a deprotonating agent then upon substitution with leucine, the mutant forms will behave differently; either there will be a dramatic change in some aspect of catalytic competence, or there will no activity and the mutant will bind sterol, AdoMet, and 25-azalanosterol to similar levels. For the latter case, the amino acid is considered important mainly to the catalytic reaction rather than to initial binding. Moreover, we hypothesized that the high energy intermediate inhibitor with an ammonium function in the sterol side chain is protonated at physiological pH and because of its charge status will bind in the AdoMet binding site rather than to the sterol binding site. The latter proposal is based on our earlier observation that 25-azalanosterol can impair SMT action with a K_i of about 25 nM (*10*, *32*). The kinetic pattern of 25-azalanosterol inhibition relative to zymosterol is noncompetitive, suggesting that it binds to a subsite in the active center other than at the sterol binding subsite. Since the 3-hydroxyl group is not essential to the 25-azasteroid inhibition of SMT action is further reason to assume the 25-azasteroids can bind in the AdoMet subsite. It is noteworthy that the K_d of 4 μM for 25-azalanosterol (Figure 2) is 2 orders of magnitude greater than its K_i of 40 nM (*32*), suggesting that upon inhibitor binding, a conformational change occurs during catalysis.

We first examined the replacement of the nine conserved acidic residues at E108, D125, D152, D189, E195, E209, E224, E246, and D276 located toward the N-terminus by sterically conservative leucine residues that are hydrophobic, electrically neutral, and spatially similar to aspartate and glutamate. In the case of D152, several SMTs possess the alternate residue D for E. Our choice for leucine screening is based on our earlier efforts that indicated that the isosteric subsitution of leucine with E82 is not disruptive to the mutant protein conformation. In the initial experiments, the activity of each purified mutant expressed in *E. coli* was determined. Two mutants at positions E108 and E246 exhibited a significant decrease (<90%) in catalytic competence (K_{cat}/K_m), and four mutants were found to be inactive at positions D125, D152, E195, and D276 (Table 2). The active mutants were tested for product outcome, and in each case, only fecosterol, the expected product, was detected by GC−MS.

The four acidic mutants for which no activity was evident were investigated further for their ability to bind sterol, AdoMet, and 25-azalanosterol. As shown in Table 2, D125 and D152 bound sterol in a manner similar to the wild-type protein, whereas E195 and D276 bound sterol weakly as compared to the wild-type SMT. The three mutants at D125, D152, and E195 bound AdoMet and 25-azalanosterol less efficiently as wild-type SMT, whereas D276 bound AdoMet and 25-azalanosterol to similar levels of the wild-type SMT. 25-Azalanosterol was bound in fashion similar to AdoMet in each of these mutants, consistent with the *C*-methylation inhibitor binding to the active center in a subsite normally occupied by AdoMet. There is a loss of ca. 3 kJ/mol of binding energy related to the AdoMet and 25-azalanosterol binding when the D125 and D152 ligands are replaced by leucine, yet there is no substantial loss of binding energy observed for the sterol substrate, suggesting for these mutants a loss of stability associated with the AdoMet binding pocket. In the case of the E195L and D276L mutants, a loss of as much as 6−8 kJ/mol binding energy is observed. For D276L, no loss of binding energy for AdoMet or 25-azalanosterol is noted, but in the case of the E195L mutant, there is an associated loss in binding energy of 3 kJ/mol for AdoMet and 25-azalanosterol binding. It is evident from these results that none of the acidic amino acids necessarily play a critical role in C-28 deprotonation since differences were observed in the binding isotherms among the substrates. Nonetheless, based on the binding data for sterol relative to AdoMet, it appears that the four acidic amino acids are involved in substrate binding; it is hypothesized that D125 and D152 are involved in AdoMet binding, and the E195 and D276 residues are involved in sterol binding. In support of our observation, D125 and 152 are conserved in the seven β-strand methyltransferase family motif I and II (in this paper, we refer to the nomenclature adopted by Blumenthal and co-workers for AdoMet-dependent methyltransferases (*25*) in contradistinction to the nomenclature of Kagan and Clarke, which refers to motif I, motif post-1 etc., ref *33*) and interact with AdoMet in these enzyme structures generally (*25*, *26*). An unexpected finding was that D189, a highly conserved residue among the SMTs, as well as other AdoMet-dependent methyltransferases as the central residue in the signature motif II of the seven-β strand class of methyltransferases (*25*), was not essential to activity. E195 can also act as a counterion to AdoMet in as yet uncharacterized catalytic triad. As these experiments were in progress, we discovered from pH profiling that another general base may be involved with catalysis, which led us to perform a second set of mutagenesis experiments involving histidine residues.

Activity Assay at Different pH Values and Site-Directed Mutagenesis of Histidine Residues. To shed light on possible amino acid residues that contribute to catalytic *C*-methylation, a pH dependence of the log k_{cat}/K_m profile was determined for SMT assayed in phosphate buffer as shown in Figure 2. The pK_a values for *C*-methylation of native enzyme are centered between 6.0 and 8.6. Plausible candidates for the immediate proton acceptor based on these data would be a deprotonated imidazole group of a histidine residue, a thiol group of cysteine, or an N-terminal amino group (pK_a values for these three amino residues = 6.5−8.5). Because the histidine side chain can exchange protons

Table 2: Kinetic Parameters and Product Distribution of Wild-Type and Mutant *ERG6* Proteins

strain	steady-state kinetic parameters[a] K_m (μM)	K_{cat} (s^{-1})	K_{cat}/K_m ($\times 10^{-4}$)	K_d ($\Delta G_{binding}$) zymosterol μM (kJ/mol)	AdoMet μM (kJ/mol)	25-azalanosterol μM (kJ/mol)	product (%) fecosterol
His90Leu	NA[b]	NA	NA	5 (−31)	3 (−32)	5 (−31)	0[d]
His107Leu	11	0.003	2.73	ND[c]	ND	ND	23
Glu108Leu	34	0.002	0.59	ND	ND	ND	34
Asp125Leu	NA	NA	NA	6 (−31)	12 (−29)	10 (−29)	0
Asp152Leu	NA	NA	NA	5 (−31)	14 (−29)	14 (−29)	0
Asp189Leu	17	0.008	4.71	ND	ND	ND	91
Glu195Leu	NA	NA	NA	42 (−26)	12 (−29)	10 (−29)	0
His199Leu	24	0.0001	0.04	ND	ND	ND	2
Glu209Leu	34	0.009	2.65	ND	ND	ND	79
Glu224Leu	17	0.008	4.71	ND	ND	ND	74
His238Leu	20	0.008	4.00	ND	ND	ND	85
Glu246Leu	42	0.002	0.48	ND	ND	ND	6
Asp276Leu	NA	NA	NA	70 (−24)	3 (−32)	5 (−31)	0
Wild type	17	0.011	6.47	4 (−32)	4 (−32)	4 (−32)	100

[a] Catalytic competence for zymosterol; parameters were measured with varied zymosterol and fixed AdoMet as described under Experimental Procedures. [b] NA: not applicable. [c] ND: not determined. [d] Product % refers to the amount of product obtained after an 18 h incubation with saturating amounts of sterol and AdoMet; 0: no product was detected at 0.1% conversion of substrate as determined by GC−MS.

near physiological pH, it often plays a role in enzymatic catalysis involving proton transfer; therefore, we chose to pursue our leucine-screening site-directed mutagenesis experiments involving the four highly conserved histidine residues at positions 90, 107, 199, and 238. Of these four histidines, only one, H90, is essential since only the H90 mutant was not active after substitution with leucine (Table 2). All three ligands, sterol, AdoMet, and 25-azalanosterol, were bound to H90L with similar efficiency as the wild-type enzyme, suggesting that H90, part of region I, acts directly in catalysis and may be responsible for the deprotonation step that generates the exomethylene structure **3**. In none of the histidine mutants that showed activity was a new product distribution detected by GC−MS; the enzyme-generated product was fecosterol. The significant decrease in catalytic competence of the H199L mutant suggests that it may also contribute to the overall reaction progress.

Structural Comparison of Wild-Type and Mutant Enzymes. Because of the lack of X-ray diffraction data for any SMT, CD is the method of choice to obtain information about the secondary structure of the native enzyme, and gel-permeation chromatography is used to reveal whether the subunit organization has been disrupted during the production or processing of the recombinant protein. Since we routinely purified the mutants from the bacteria expression system, the amount of protein for characterization by spectral and chromatographic methods was similar. The pure H90L mutant was compared to the wild-type enzyme. As revealed in the gel-permeation chromatograms (Figure 3) and CD spectra (Figure 4) taken on the native protein (Figure 3A) and H90L mutant (Figure 3B), no major difference was detected between the H90L mutant and the wild-type enzyme. Structure estimation according to CD measurements indicated for the wild-type and mutant enzymes the following populations of structures: 43 and 50% α-helix, 29 and 24% β-sheet, 7 and 3% turn, and 21 and 23% random coil, respectively; and as shown in Figure 5, the overall secondary structures for the mutant and wild-type enzymes were similar. The other mutants were tested in similar fashion and found to be comparable to the wild-type enzyme within the limits of the CD and gel-permeation chromatographic methods

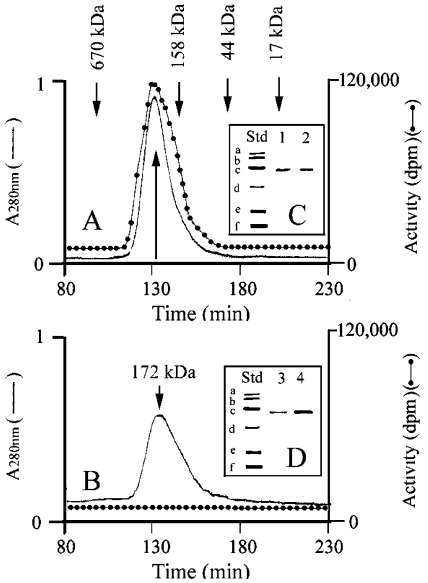

FIGURE 3: Gel-permeation chromatography of wild-type (A) and H90L mutant (B) enzymes of *S. cerevisiae* SMTs. Protein as measured by the absorption at A_{280} (—) and SMT activity assay (●) are plotted. The standard migrating at 310 min corresponding to 1.3 kDa is not shown. The chromatographic fraction corresponding to peak protein concentration was monitored by Coomasssie blue staining of SDS−PAGE gels (1 and 3, inset) and by Western blot (2 and 4, inset). The migration of protein standards (in kDa) are indicated; a, 97.4; b, 66.2; c, 45.0; d, 31.0; e, 21.5; and f, 14.4.

(data not shown). Thus, these investigations revealed that, except for changes in activity, the mutations did not result in significant changes in secondary structure. This is the first report of the CD spectra of a SMT from any source; no information is available concerning structural details of SMT enzymes.

Homology Modeling with SMT. There is no X-ray data for a SMT enzyme. Since the SMT is a AdoMet-dependent enzyme, to generate a working topology diagram of the *ERG*6 SMT in which the putative location of the cosubstrates can be viewed, we searched the protein database for three-dimensional structures of enzymes of related enzymes that utilize AdoMet as the methyl group donor. There are more than 30 AdoMet-dependent enzymes for which crystal

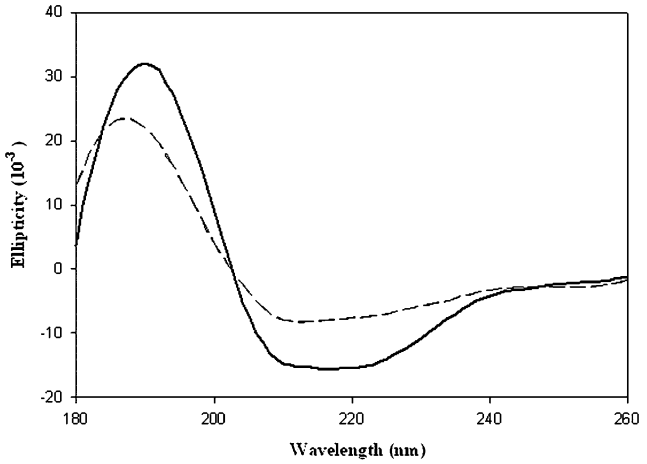

FIGURE 4: Far-UV CD spectrum of wild-type yeast SMT. The CD spectrum of H90L mutant yeast SMT is shown by overlay as a dotted line. The CD spectra were recorded as described under Experimental Procedures.

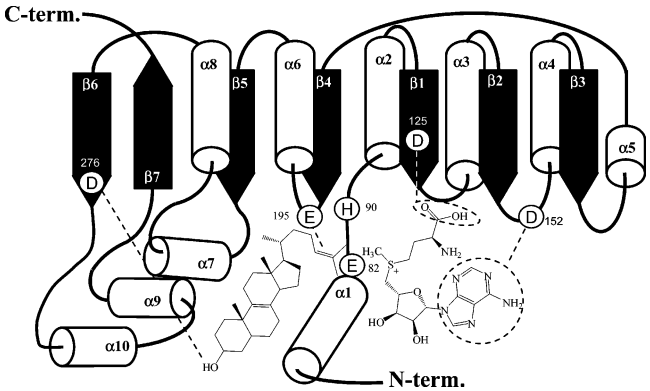

FIGURE 5: Schematic representation of the methyltransferase fold of the SMT; spatial arrangement of the secondary structure elements in relation to sterol and AdoMet substrates. The structure of SMT is predicted based on known crystallographic structures of AdoMet-dependent methyltransferase detected by the fold-recognition analysis (*25*, *27*), sequence alignment data for 16 SMTs shown in the Supporting Information, and structure−activity assays of sterol substrates tested with SMTs (*16*, *29*, *32*).

structures exist in the literature (refs *25* and *26* and references therein). Most of them (class I methyltransferase) show a similar α/*β* Rossmann-like fold with a central parallel *β*-sheet surrounded by α-helices. The fold-recognition analysis carried out via the Meta server (*27*) revealed significant similarity of the SMT to the structures of class I methyltransferases. These structures were subsequently used as templates to model the secondary and tertiary structure of the SMT. The population of α-helices to *β*-sheets estimated from homology modeling is comparable to the population of these structures determined by CD spectroscopic measurements. Structural analysis and sequence alignment of the SMT and related AdoMet-dependent enzymes revealed a set of motifs that interact with AdoMet. The conserved tertiary topology of the AdoMet binding fold and equivalence of the order and spacing of the AdoMet motifs among these enzymes as well as knowledge about the sterol binding pocket for the *ERG*6 SMT allow for the prediction of the relation of sterol and AdoMet in the active center as shown in Figure 5. There is good agreement of homology modeling and the CD spectra with respect to α-helical contents. The relative contributions of *β*-sheet and random coil do not agree as well, and a detailed analysis must await the X-ray determination of the SMT structure.

CONCLUSIONS

All SMTs are considered to catalyze similar overall reactions (Scheme 2) involving binding the substrate in appropriate conformation(s), initiating the *C*-methylation reaction, channeling the conformations of reactive intermediates through directed side chain orientations, and terminating the *C*-methylation by deprotonation. The sequence homology and well-conserved region I between yeast SMT and other fungal and plant SMTs implicate the strongly conserved structural and mechanistic similarities. Analysis of homology modeling of the SMT and structure−function relationships using the wild-type and mutant proteins from yeast described in this and our other recent papers (*16*, *19*, *20*) and consideration of AdoMet interactions with AdoMet-dependent enzymes discussed elsewhere (*25*, *26*) suggest a common set of interactions at initial binding between substrates and SMT. Taken together, (i) the acidic amino acids at D125 and D152 form a wall of the AdoMet binding site, perhaps hydrogen bonding to the methionine and ribose moieties of the substrate, (ii) D276 and E195 are positioned to hydrogen bond directly or by way of a water bridge to the proximal (C-3 hydroxyl group) and distal (Δ^{24}-bond) nucleophilic segments of the sterol molecule, respectively. Indeed, distinct

Scheme 2: Hypothetical Steric−Electric Plug Model for Substrate Binding and Catalysis by the Yeast SMT (*1*)

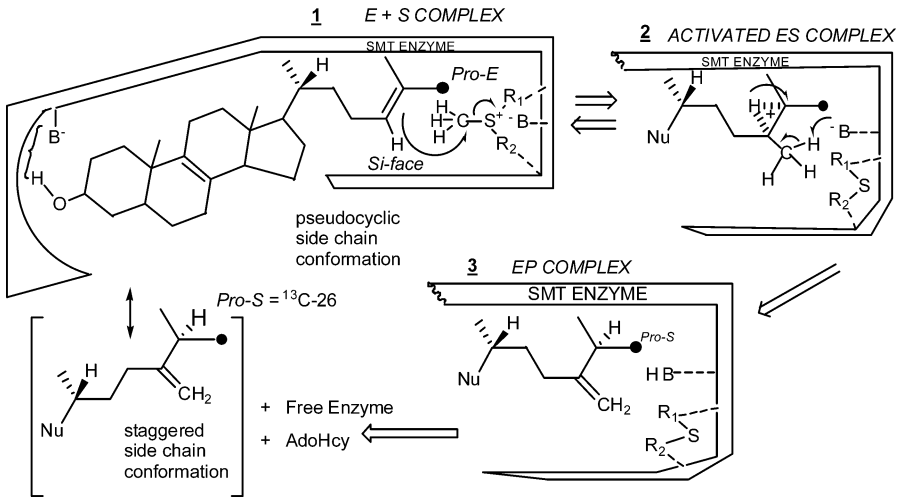

bases were predicted (steric−electric plug model (*28*, *29*)) to anchor sterol in the ternary complex based on structure−function tests involving a series of substrate analogues assayed with different SMTs (Figure 5). E195 may also interact with the positive charge on the sulfur residue of AdoMet, in which case it may serve as the elusive counterion to AdoMet, (iii) H90, positioned above (*Si*-face) the substrate double bond in the same plane as AdoMet, may serve as the base involved with C-28 deprotonation that leads CH_3 **2** to CH_2 **3** production, and (iv) the high energy intermediate analogue 25-azalanosterol binds to the active center. This knowledge may help in the design of more potent and selective inhibitors of SMT activity.

SUPPORTING INFORMATION AVAILABLE

Alignment of deduced amino acid sequences. This material is available free of charge via the Internet at http://pubs.acs.org.

REFERENCES

1. Nes, W. D. (2000) *Biochim. Biophys. Acta 1529*, 63−88.
2. Nes, W. R., Sekula, B. C., Nes, W. D., and Adler, J. H. (1978) *J. Biol. Chem. 253*, 6218−6225.
3. Bloch, K. E. (1983) *CRC Crit. Rev. Biochem. 14*, 47−92.
4. Welihinda, A. A., Beavis, A. D., and Trumbly, R. J. (1994) *Biochim. Biophys. Acta 1193*, 107−117.
5. Jensen-Pergakes, K. L., Kennedy, M. A., Lees, N. D., Barbuch, R., Koegel, C., and Bard, M. (1998) *Antimicrobiol. Agents Chemother. 42*, 1160−1167.
6. Nes, W. D., McCourt, B. S., Zhou, W.-X., Ma, J., Marshall, J. A., Peek, L.-A., and Brennan, M. (1998) *Arch. Biochem. Biophys. 353*, 297−311.
7. Kaneshiro, E. S. (2002) *Drug Res. Updates 5*, 259−268.
8. Georgopapadakou, N. H. (1998) *Curr. Opin. Microbiol. 1*, 547−557.
9. Guo, D., Mangla, A. T., Zhou, W., Lopez, M., Jia, Z., Nichols, D., and Nes, W. D. (1997) *Subcellular Biochem. 8*, 89−118.
10. Oehleschlager, A. C., Angus, R. H., Pierce, A. M., Pierce, H. D., and Srinivasan, R. (1984) *Biochemistry 23*, 3582−3589.
11. Nes, W. D., Xu, S., and Parish, E. J. (1989) *Arch. Biochem. Biophys. 272*, 323−331.
12. Beuchet, P., Dherbomez, L., Charles, E. G., and Letourneux, Y. (1999) *Bioorg. Med. Chem. Lett. 9*, 1599−1600.
13. Conteras, L. M., Viva, J., and Urbina, J. A. (1997) *Biochem. Pharmacol. 53*, 697−704.
14. Chung, S.-K., Ryoo, C. H., Yang, H. W., Shim, J.-Y., Kang, M. G., Lee, K. W., and Kang, H. I. (1998) *Tetrahedron 54*, 15899−15914.
15. Urbina, J. A., Visba, G., Coneras, L. M., McLaughlin, G., and Docampo, R. (1997) *Antimicrobiol. Agents Chemother. 41*, 1428−1432.
16. Nes, W. D. (2003) *Phytochemistry 64*, 75−95.
17. Nes, W. D., Song, Z., Dennis, A. L., Zhou, W., Nam, J., and Miller, M. B. (2003) *J. Biol. Chem. 278*, 34505−34516.
18. Zhou, W., and Nes, W. D. (2003) *Arch. Biochem. Biophys. 420*, 18−34.
19. Nes, W. D., Marshall, J. A., Jaradat, T. T., Song, Z., and Jayasimha, P. (2002) *J. Biol. Chem. 277*, 42549−42556.
20. Nes, W. D., McCourt, B. S., Marshall, J. A., Ma, J., Dennis, A. L., Lopez, M., Li, H., and He, L. (1999) *J. Org. Chem. 64*, 1535−1542.
21. Le, P. H., and Nes, W. D. (1986) *Chem. Phys. Lipids 40*, 57−69.
22. Bradford, M. M. (1976) *Anal. Biochem. 72*, 248−254.
23. Copeland, R. A. (2000) *Enzymes; A practical Introduction to Structure, Mechanism, and Data Analysis*, 2nd ed., John Wiley & Sons, Inc., New York.
24. Sreerema, N., and Woody, R. W. (2000) *Anal. Biochem. 287*, 252−260.
25. Fauman, E. B., Blumenthal, R. M., and Cheng, X. (1999) *S-Adenosyl-L-methionine-Dependent Methyltransferase: Structure and Functions*, pp 1−38, World Scientific Co., Singapore.
26. Kosinski, J., Cymerman, I. A., Feder, M., Kurowski, M. A., Sasin, J. M., and Bujnicki, J. M. (2003) *Proteins, 53* (CASP-5, special issue).
27. Kurowski, M. A., and Bujnicki, J. M. (2003) *Nucleic Acid Res. 31*, 3305−3307.
28. Nes, W. D., Janssen, G. G., and Bergenstrahle, A. (1991) *J. Biol. Chem. 266*, 15202−15212.
29. Parker, S. R., and Nes, W. D. (1992) *Am. Chem. Soc. Symp. Ser. 497*, 110−145.
30. Rahier, A., Genot, J.-C., Schuber, F., Benveniste, P., and Narula, A. S. (1984) *J. Biol. Chem. 259*, 15215−15223.
31. Arigoni, D. (1978) *Ciba Found. Symp. 60*, 242−261.
32. Venkatramesh, M., Guo, D., Jia, Z., and Nes, W. D. (1996) *Biochim. Biophys. Acta 1299*, 313−324.
33. Kagan, R. M., and Clarke, S. (1994) *Arch. Biochem. Biophys. 310*, 417−427.

BI035257Z